Asian Journal of Chemistry; Vol. 26, No. 9 (2014), 2632-2636

ASIAN JOURNAL OF CHEMISTRY

http://dx.doi.org/10.14233/ajchem.2014.15771

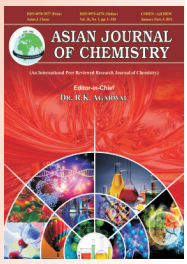

Synthesis and Electrochemical Properties of Hexagonal Sliced $LiNi_{0.5}Mn_{0.5}O_2$ as Cathode Materials for Li-ion Batteries

SHUMEI DOU[1,*] and QING LI[2]

[1]Department of Chemistry and Chemical Engineer, Baoji University of Arts and Sciences, Baoji 721013, Shaanxi, P.R. China
[2]Baoji Middle School, Baoji 721013, Shaanxi, P.R. China

*Corresponding author: Tel: 86 917 3566589; E-mail: dsmwxsh@163.com

Received: 15 May 2013; *Accepted*: 13 September 2013; *Published online*: 28 April 2014; AJC-15085

Single-phase lithium nickel manganese oxide, $LiNi_{0.5}Mn_{0.5}O_2$, was successfully synthesized from nickel manganese oxide precursor that prepared by co-precipitation step by step. SEM images show the final product $LiNi_{0.5}Mn_{0.5}O_2$ has a uniform morphology composed of hexagonal cubes with the diameter about 300 nm composed of hexagonal slices and smooth crystal surface. The measured cation ratios of Ni: Mn in different sites is nearly 1:1 according to the results of EDAX. X-ray diffraction pattern shows that the product is well crystallized with a high value of I_{003}/I_{104} and no diffraction peaks of $LiMn_2O_3$ can be detected. Electrochemical performance of as-prepared $LiNi_{0.5}Mn_{0.5}O_2$ was examined in the test battery by charge-discharge cycling with different rate. The cycling behavior between 2.5 and 4.4 V at a current rate of 20 mA g^{-1} shows a reversible capacity of about 209 mAh g^{-1} with little capacity fading after 30 cycles. High-rate capability test shows that even at a rate of 320 mA g^{-1}, stable capacity about 108 mAh g^{-1} is still retained. The favorable electrochemical performance was primarily attributed to regular and stable crustal structure with the uniform morphology.

Keywords: Lithium-ion battery, $LiNi_{0.5}Mn_{0.5}O_2$, Hexagonal sliced structure, Co-precipitation step by step, Electrochemical property.

INTRODUCTION

During the past decades, due to the much higher energy and higher power density per unit compared to other rechargeable battery systems, lithium ion batteries have been predominated in the portable energy storage devices. Now, they are being intensively required not only to enable the moderately charge/discharge rates applications like mobile phone and portable computer but also to meet an increasing need for new applications such as hybrid electric vehicles (HEV), plug-in hybrid electric vehicles (PHEV) and electric vehicles (EV), which need power sources with both high energy and high power density, as well as considered for stationary storage and utilization of intermittent renewable energies like solar and wind. Lithium-ion batteries for these on-going applications are depending on the cost, safety, charge/discharge rate, cycle life, energy and power, which are mainly controlled by the components used in batteries[1,2]. Compared to the anode materials, cathode materials have some disadvantages, such as lower voltage, more inferior capacity, *etc*. Therefore, looking for the cathode materials to be provided with elevated voltage, high capacity, good cycle performance, safe and low cost, has become one of the focus topics in recent years.

Both $LiNi_{0.5}Mn_{0.5}O_2$ and $Li[Ni_xLi_{(1/3-2x/3)}Mn_{(2/3-x/3)}]O_2$ synthesized above the temperature of 800 °C, reported by Ohzuku and Makimurd[3] and Dahn *et al.*[4] showing the prominent performance of the electrochemical properties. Since then, the lithium nickel manganese oxides have caused great concerns in the field of academy. Various synthesis method such as solid-state reaction[3, 5-9], ion-exchange [6,10], hydroxide co-precipitation method[4,11,12], hydrothermal synthesis[13], ultrasonic assistance synthesis[14], layered-spinel composite cathode system[15] *etc.*, have been applied to prepare these system materials. However, the lithium nickel manganese oxides synthesized with these methods are not higher battery-active due to either containing substantial Li/Ni disorder or existing structure impurity. Recently, there are two major breakthrough in solving those problems that is either to transform solid solution of $Ni_{1.5}Mn_{1.5}O_4$ into $Li(Ni_{0.5}Mn_{0.5})O_2$ by the solid reaction[8], or to synthesize concerntration-gradient cathode material[16]. The former is one of the effective ways to decrease the substantial Li/Ni disorder, showing that the as-prepared $LiNi_{0.5}Mn_{0.5}O_2$ material has good electrochemical reversibility and structure stability. For the latter, the central bulk that is rich in Ni can provides high capacity whereas the Mn-rich outer layer can improve the thermal stability, suggesting that meet the demanding performance and safety requirements of hybrid electric vehicles.

Furthermore, Yang *et al.*[17] synthesized a spherical lithium-rich layered cathode material $Li_{1.13}[Mn_{0.534}Ni_{0.233}Co_{0.233}]_{0.87}O_2$ by co-precipitation, which was consisted of an inner core and a stable concentration-gradient outer layer in which manganese content was gradually increased. In this material, a typical rhombohedral $LiNiO_2$-like layered structure with the existence of the monoclinic Li_2MnO_3-type intergrated component can be detected. The lithium-rich layered material can deliver a high capacity of 220 mAh g^{-1} and the excellent cycle life and improved thermal stability were achieved by the concertration-gradient out layer. This inspired us to prepare cathode material for lithium-ion batteries with this step-by-step co-precipitation.

In this work, we report on hexagonal cube structured $LiNi_{0.5}Mn_{0.5}O_2$ material assembled by hexagonal sliced as the cathode material for rechargeable lithium-ion batteries. The formation of hexagonal cubes structred $LiNi_{0.5}Mn_{0.5}O_2$ was inherited from nickel manganese oxides nanoparticles which were obtained from the co-precipitation method by three steps. The results of electrochemical measurements indicate that the cathode material made of hexagonal cubes structured $LiNi_{0.5}Mn_{0.5}O_2$ exhibits a large capacity and excellent cycling stability.

EXPERIMENTAL

Synthesis of $LiNi_{0.5}Mn_{0.5}O_2$ material: The preparation of hexagonal cubes structured $LiNi_{0.5}Mn_{0.5}O_2$ material follows a two steps route. First, nickel manganese oxide nanoparticles was produced by a simple co-precipitation method using $NiCl_2{\cdot}6H_2O$ and $MnCl_2{\cdot}4H_2O$ as the sources, $LiOH{\cdot}H_2O$ as the precipitants. Initially, 250 mL de-ionized water was taken as a base solution. The pH value of the base solution was adjusted to 8 with a few drops of ammonia and then the base solution was fed into a reactor $NiCl_2{\cdot}6H_2O$ and $MnCl_2{\cdot}4H_2O$ (8:2 molar ratio) were dissolved in de-ionized water to get a 2 M aqueous solution. Then, the chloride solution, a desired amount of ammonia solution and 6 M $LiOH{\cdot}H_2O$ solution were fen into the reactor with vigorous stirring. After reaction for 2 h, a 2 M aqueous solution of $NiCl_2{\cdot}6H_2O$ and $MnCl_2{\cdot}4H_2O$ (5:5 molar ratio) was pumped into the reactor and the desired amount of ammonia solution and 6 M $LiOH{\cdot}H_2O$ solution were fen into the reactor drop by drop. After reaction for 2 h, a 2 M aqueous solution of $NiCl_2{\cdot}6H_2O$ and $MnCl_2{\cdot}4H_2O$ (2:8 molar ratio) was pumped into the reactor and repeat the above operation. All of the above steps are carried out under nitrogen protection. The precipitate was filtered washed and dried at 70 °C in a vacuum oven. The precursor powder was mixed with stoichiometric $LiOH{\cdot}H_2O$ (5 m % excess) thoroughly, preliminarily annealed at 480 °C for 3h to dissolve fully and finally calcined at 850 °C for 12 h in a tube furnace in air to get the hexagonal cubes structured material.

X-ray diffraction (XRD) patterns were recorded on a Philips X 'Pert spectrometer using CoK_α radiation ($\lambda = 1.78897$ Å) and the data were converted to CuK_α data. Scanning electron microscopy (SEM), energy dispersive X-ray analysis (EDAX) and transmission electron microscopy (TEM) images were taken on a Horiba Ex-250 instrument and a Tecnai G2 F20 instrument, respectively.

Electrochemical tests: Charge and discharge profiles were collected by galvanostatically cycling between 2.5 and 4.4 V (Shenzhen Neware, BTS, China). For the preparation of cathode sheets, slurry was formed by mixing the active material, acetylene black and binder (polyvinylideneuoride, dissolved in N-methyl-2-pyrrolidone) in a weight ratio of 75:20:5. The slurry was spread uniformly on aluminium foil. The electrodes were dried under vacuum at 120 °C for 10 h and then pressed under 60 MPa and weighted. 1 M $LiPF_6$ in a 1:1 ethylene carbonate/diethyl carbonate was used as electrolyte and lithium foil was used as anode. A thin sheet of microporous polypropylene insulated the positive electrode from negative electrodes. Battery assembly was carried out in an argon-filled glove box.

RESULTS AND DISCUSSION

Fig. 1 illustrates the XRD pattern of the as-prepared nickel manganese oxide precursor by co-precipitation method. All the peaks in Fig.1 can be indexed to the mixed phase of various nickel manganese oxides including $NiMn_2O_4$ and $MnNi_2O_4$ and α-MnO_2/NiO can be observed owing to the complicated preparation which different molar ratio of $NiCl_2{\cdot}6H_2O$ and $MnCl_2{\cdot}4H_2O$ pumped into the reactor in a different order. The broadening of XRD peaks suggests the small crystallite sizes of the obtained nickel manganese oxide precursor. Up to now, we still could not judge the precisely phase of the powder. The morphologies of the precursor are characterized by SEM measurements. Figs. 2 and 2a show that the precursor powder takes on nanoparticles with size of less than 10 nm from the high magnified image of (Fig. 2b).

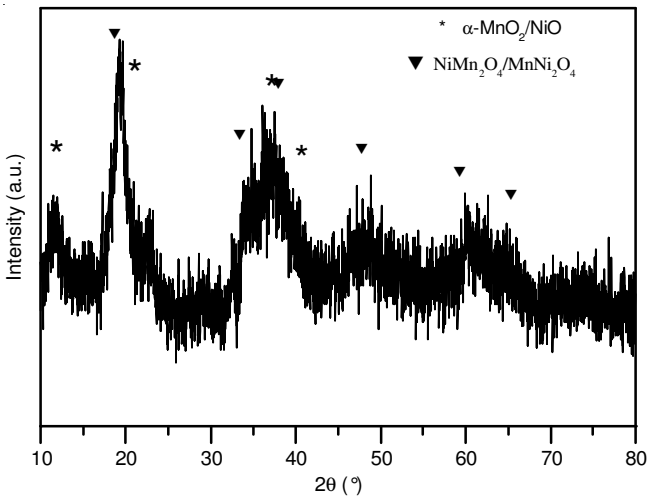

Fig. 1. XRD pattern of the as-prepared nickel manganese oxide precursor

The chemical compositions of the prepared powders were determined by the EDAX. The patterns of the EDAX are shown in Figs. 2c & 2d by selecting the different site of 1, 2 in Fig. 2b and the results are summarized in Table-1. The measured cation ratios of Ni:Mn in different sites is well in agreement to the intended composition, which implies that the metal oxides are homogenously reacted.

Fig. 3 shows the XRD pattern of the as-synthesized $LiNi_{0.5}Mn_{0.5}O_2$ prepared by reaction of nickel manganese oxide nanoparticle and LiOH at 850 °C for 12 h. All the diffraction peaks can be indexed with the α-$NaFeO_2$-type structure with space group R-3m and scarcely any sigh of the undesired $LiMn_2O_3$ can be found under the detection limitation[13,18].

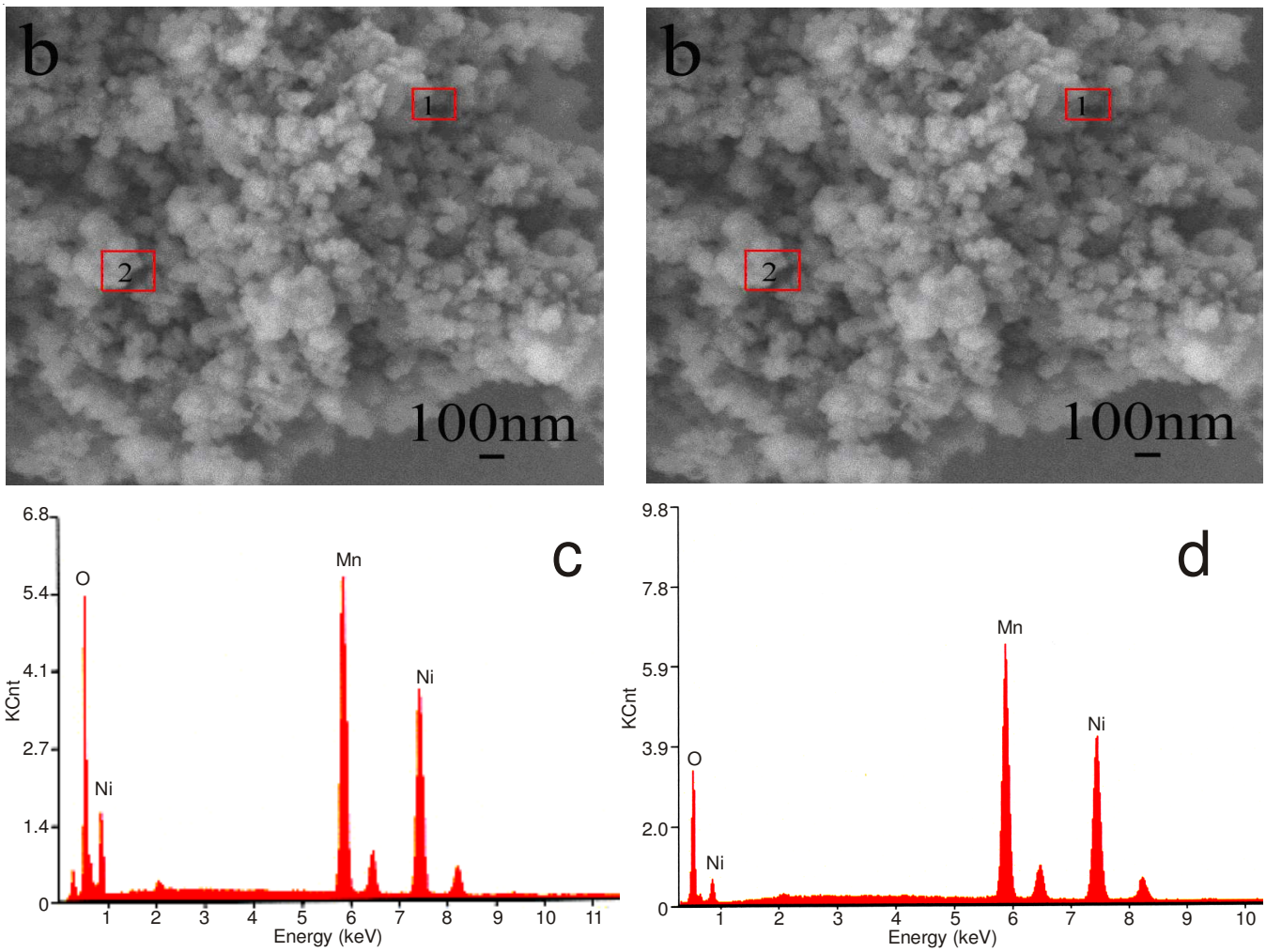

Fig. 2. SEM images of the nickel manganese oxide precursor (a, b) and (c, d) corresponding EDAX patterns of the sites (1) and (2) in (b), respectively

TABLE-1
CHEMICAL COMPOSITION (AT %) OF THE PREPARED PRECURSOR AND PRODUCT DETERMINED BY EDAX CORRESPONDING TO THE SITE OF 1, 2 AND 3,4 IN FIGURE 2b AND 4b, RESPECTIVELY

At %	1	2	3	4
Mn	17.71	23.81	14.62	21.27
Ni	18.30	23.04	14.05	21.08

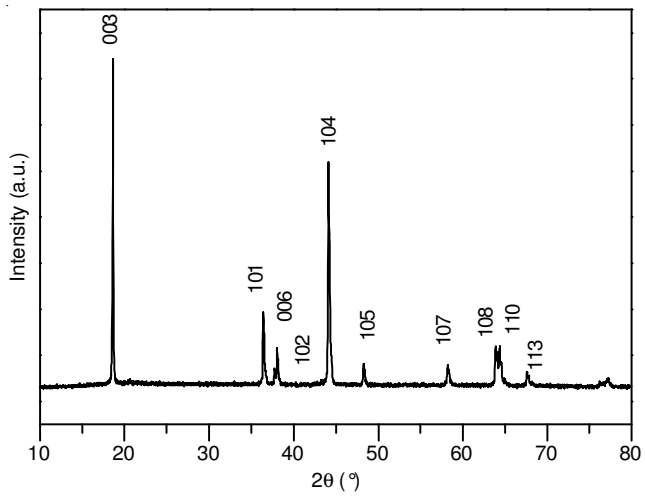

Fig. 3. XRD pattern of the core-shell structured $LiNi_{0.5}Mn_{0.5}O_2$

Moreover, the final product calcined at 850 °C shows good crystallinity of the material because of the narrow XRD peaks. Lattice parameters obtained from ten $LiNi_{0.5}Mn_{0.5}O_2$ samples with the identical electrochemical reactivity are a = 2.891 Å and c = 14.18 Å in a hexagonal. Both the c/a (4.91) and the I_{003}/I_{104} (1.36) intensity ratio indicate a high degree of the Li-Ni order in their respective layers. The splitting of the (006)/(102) and (108)/(110) diffraction pairs can be clearly detected, indicating that the product of $LiNi_{0.5}Mn_{0.5}O_2$ is almost ideal layered structure and crystallinity.

Fig. 4a gives the SEM images of the finally product $LiNi_{0.5}Mn_{0.5}O_2$ that has a uniform morphology composed of hexagonal cubes with the diameter about 300 nm and smooth crystal surface. And the hexagonal cubes are composed of hexagonal slices from the extended images of (Fig. 4b). The chemical compositions of the prepared powders determined by the EDAX are shown in Figs. 2c & 2d by selecting the different site of 3, 4 in Fig. 4b and the results are summarized in Table-1. The measured cation ratios of Ni: Mn in different sites is well in agreement to the intended composition, which implies that the metal oxides are homogenously reacted.

The initial, 2nd, 3rd, 5th, 10th, 20th and 30th cycle charge-discharge curves of $LiNi_{0.5}Mn_{0.5}O_2$ are shown in Fig. 4a. The cell was operated in the voltage range from 2.5 to 4.4 V at a

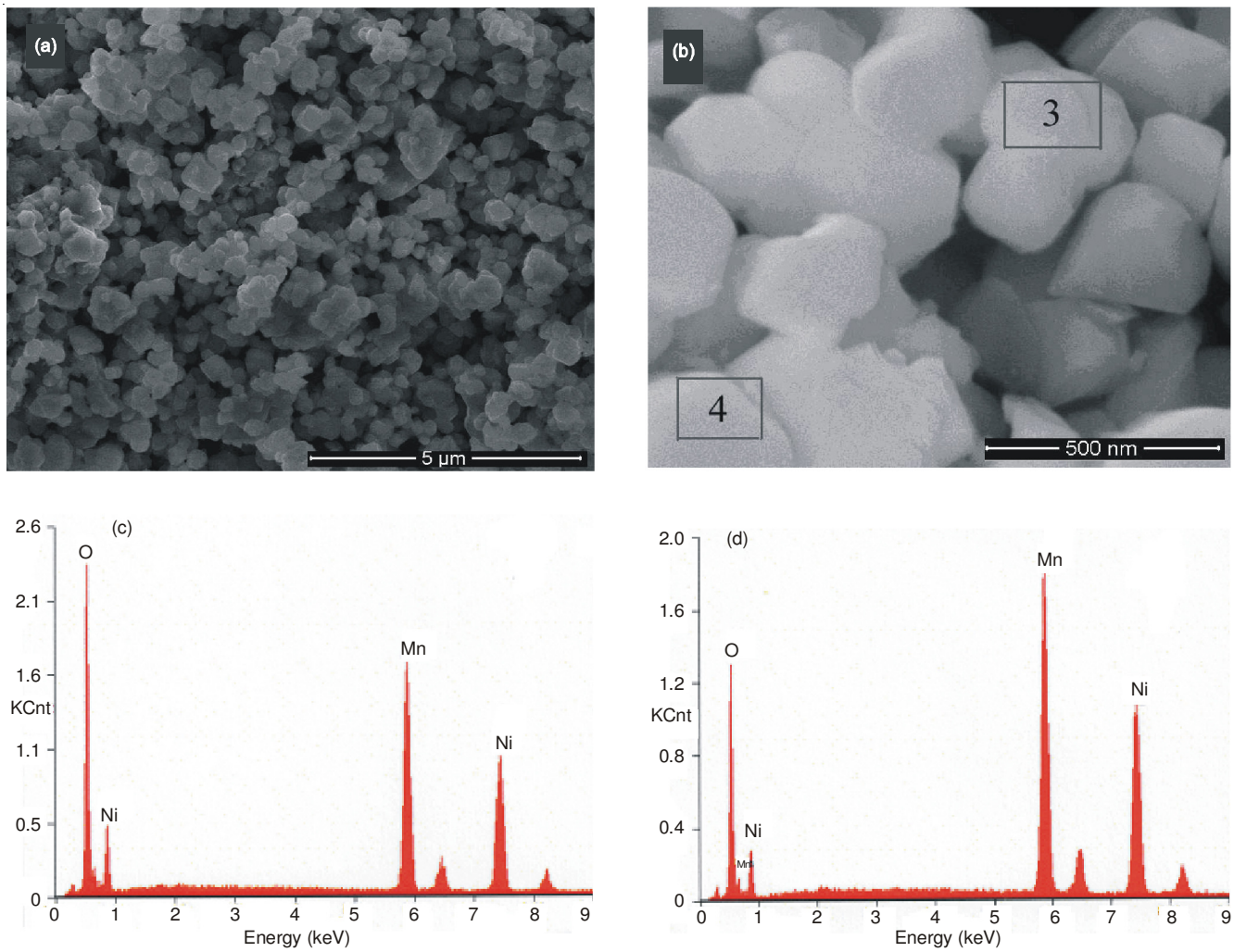

Fig. 4. SEM images of the finally production $LiNi_{0.5}Mn_{0.5}O_2$ (a, b) and (c, d) corresponding EDAX patterns of the sites (3, 4) in (b), respectively

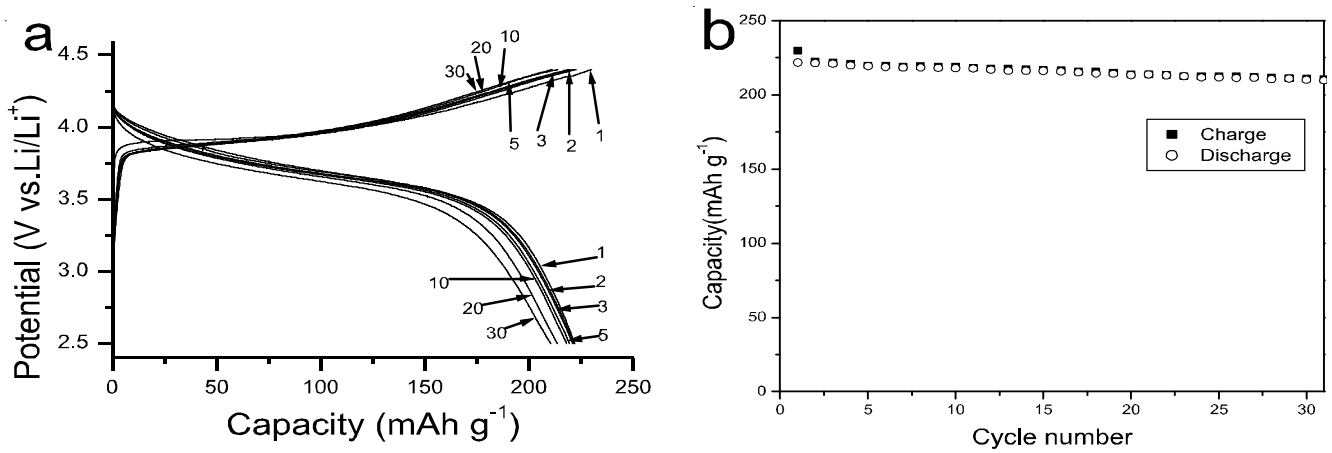

Fig. 5. (a) charge and discharge curves of the synthesized $LiNi_{0.5}Mn_{0.5}O_2$ in the voltage from 2.5 to 4.4 V at a rate of 20 mA g^{-1}, (b) charge and discharge capacity as a function of cycle number

current rate of 20 mA g^{-1}. There is only one voltage plateau on both charge and discharge curves. The ratio of initial discharge/charge is about 96 %. From the 2nd to the 30th cycles, the ratios of discharge/charge are larger than 98 %, illuminating that the electrochemical reversibility was established after the initial cycle. As shown in Fig. 6b, the batteries capacity fading during 30 cycles, with only 5 % capacity decreased. This result indicates that the designed cathode about 209 mAh g^{-1} of rechargeable capacity without dramatic material with high capacity has a high degree of cation ordering required for good Li^+ mobility.

In addition, we focus on the durability on the constant current charge/discharge measurement by different rates over the voltage range of 2.5-4.4 V and the results are shown in Fig. 5a. The first discharge capacities of the $LiNi_{0.5}Mn_{0.5}O_2$ are 221, 210, 172, 137 and 142 mAh g^{-1} at 20, 40, 80, 160 and 320 mA g^{-1}, respectively. It is notable that the capacity retention

rate at 320 mA g^{-1} maintained nearly 65 % of its capacity compared with 20 mA g^{-1}. Fig. 5b compares the rate capability of the $LiNi_{0.5}Mn_{0.5}O_2$ with charge/discharge rate of 20 mA g^{-1} to 320 mA g^{-1}, showing obviously slow capacity decay with increasing discharge rate. After 30 cycles with the discharge rate of 320 mA g^{-1}, the discharge capacity is still maintained 108 mAh g^{-1}. The good capacity retention for the synthesized $LiNi_{0.5}Mn_{0.5}O_2$ after cycling at constant charge/discharge rate suggests that its structure is stable (Fig. 6).

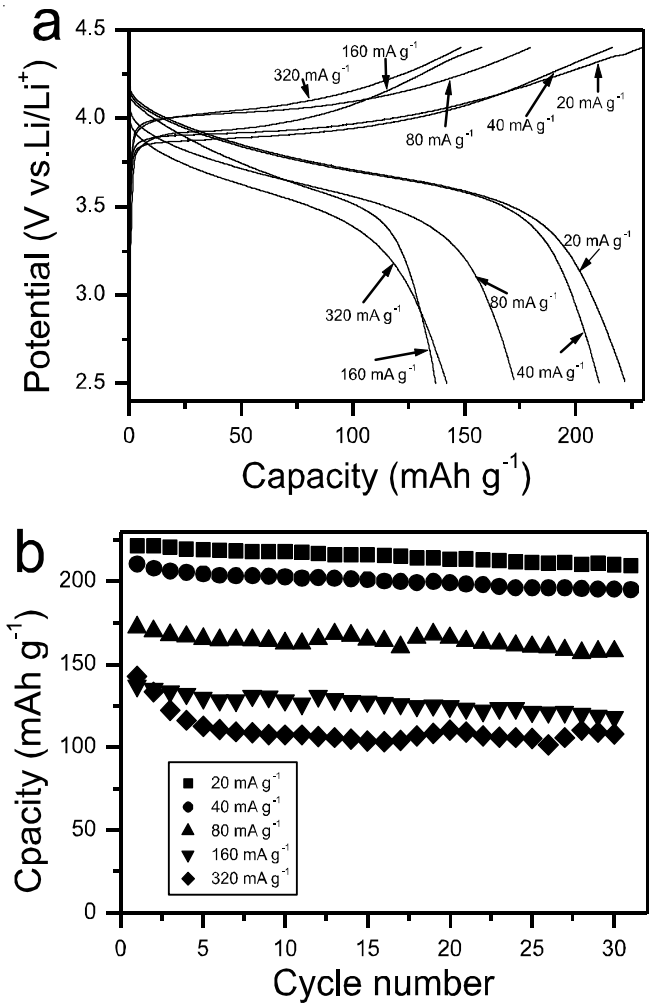

Fig. 6. (a) charge and discharge curves of the $LiNi_{0.5}Mn_{0.5}O_2$ at different current rate, (b) discharge capacity at different current rate as a function of cycle number

Conclusion

In summary, layered $LiNi_{0.5}Mn_{0.5}O_2$ compounds have been prepared with the nickel manganese oxide nanoparicles precursor synthesized by co-precipitation by three steps under the protection of nitrogen. The presence of hexagonal cubes with diameter about 300 nm composed of hexagonal slices and the distribution of nickel and manganese are confirmed by SEM and EDAX. When applied as cathode materials for rechargeable lithium-ion batteries, the hexagonal cubes structured $LiNi_{0.5}Mn_{0.5}O_2$ revealed stable high-rate capability. The discharge capacity is 108 mAh g^{-1} at the current rate of 320 mA g^{-1} and it shows good capacity retention after 30 cycles. The excellent high rate for hexagonal cubes structured $LiNi_{0.5}Mn_{0.5}O_2$ maybe due to its sliced morphology which is suitable for lithium ion diffusion. It is believed that this synthetic method would be easily extended to large-scale production. The simple synthesis method and the excellent electrochemical properties indicate that the synthesized $LiNi_{0.5}Mn_{0.5}O_2$ can be used as a possible alternative to $LiCoO_2$ in responsed to an expanding need for the advanced lithium-ion batteries.

ACKNOWLEDGEMENTS

This work was supported by the doctor initial foundation of Baoji University of arts and sciences (ZK1052) and Bamboo shoots plan of Shaanxi.

REFERENCES

1. J.-M. Tarascon, Philos. *Trans. R. Soc. London, Ser. A*, **368**, 3227 (2010).
2. A. Manthiram, *J. Phys. Chem. Lett*., **2**, 176 (2011).
3. T. Ohzuku and Y. Makimura, *Chem. Lett*., 744 (2001).
4. Z.H. Lu, D.D. Macneil and J.R. Dahn, *Electrochem. Solid-State Lett*., **4**, A191 (2001).
5. Y. Makimura and T. Ohzuku, *J. Power Sources*, **119–121**, 156 (2003).
6. K. Kang, Y.S. Meng, J. Breger, C.P. Grey and G. Ceder, *Science*, **311**, 977 (2006).
7. H. Xia, S.B. Tang and L. Lu, *J. Alloys Comp*., **449**, 296 (2008).
8. X.L. Meng, S.M. Dou and W.L. Wang, *J. Power Sources*, **184**, 489 (2008).
9. S.J. Shi, J.P. Tu, Y.Y. Tang, Y.Q. Zhang, X.L. Wang and C.D. Gu, *J. Power Sources*, **240**, 140 (2013).
10. Y. Hinuma, Y.S. Meng, K. Kang and G. Ceder, *Chem. Mater*., **19**, 1790 (2007).
11. Z. Lu, L.Y. Beaulieu, R.A. Donaberger, C.L. Thomas and J.R. Dahn, *J. Electrochem. Soc*., **149**, A778 (2002).
12. H.-J. Noh, S. Youn, C.S. Yoon and Y.-K. Sun, *J. Power Sources*, **233**, 121 (2013).
13. J. Cho, Y. Kim and M.G. Kim, *J. Phys. Chem. C*, **111**, 3192 (2007).
14. B. Zhang, G. Chen, P. Xu and Z. Lv, *Solid State Ion*., **178**, 1230 (2007).
15. E.-S. Lee, A. Huq and A. Manthiram, *J. Power Sources*, **240**, 193 (2013).
16. Y.-K. Sun, S.-T. Myung, B.-C. Park, J. Prakash, I. Belharouak and K. Amine, *Nat. Mater*., **8**, 320 (2009).
17. X. Yang, X. Wang, G. Zou, L. Hu, H. Shu, S. Yang, L. Liu, H. Hu, H. Yuan, B. Hu, Q. Wei and L. Yi, *J. Power Sources*, **232**, 338 (2013).
18. H. Xia, S.B. Tang and L. Lu, *J. Alloys Comp*., **449**, 296 (2008).